The Astrophysical Journal Letters, 720:L62–L66, 2010 September 1 doi:10.1088/2041-8205/720/1/L62

THE SPHERICALIZATION OF DARK MATTER HALOS BY GALAXY DISKS

Stelios Kazantzidis[1,2,3], Mario G. Abadi[4], and Julio F. Navarro[5]
[1] Center for Cosmology and Astro-Particle Physics, The Ohio State University, Columbus, OH 43210, USA; stelios@mps.ohio-state.edu
[2] Department of Physics, The Ohio State University, Columbus, OH 43210, USA
[3] Department of Astronomy, The Ohio State University, Columbus, OH 43210, USA
[4] Instituto de Astronomía Teórica y Experimental (IATE), Observatorio Astronómico de Córdoba and CONICET, Laprida 854 X5000BGR Córdoba, Argentina; mario@oac.uncor.edu
[5] Department of Physics and Astronomy, University of Victoria, 3800 Finnerty Road, Victoria, BC V8P 5C2, Canada; jfn@uvic.ca
Received 2010 June 3; accepted 2010 July 27; published 2010 August 11

ABSTRACT

Cosmological simulations indicate that cold dark matter (CDM) halos should be triaxial. Validating this theoretical prediction is, however, less than straightforward because the assembly of galaxies is expected to modify halo shapes and to render them more axisymmetric. We use a suite of *N*-body simulations to quantitatively investigate the effect of the growth of a central disk galaxy on the shape of triaxial dark matter halos. In most circumstances, the halo responds to the presence of the disk by becoming more spherical. The net effect depends weakly on the timescale of the disk assembly but noticeably on the orientation of the disk relative to the halo principal axes, and it is maximal when the disk symmetry axis is aligned with the major axis of the halo. The effect depends most sensitively on the overall gravitational importance of the disk. Our results indicate that exponential disks whose contribution peaks at less than ∼50% of their circular velocity are unable to noticeably modify the shape of the gravitational potential of their surrounding halos. Many dwarf and low surface brightness galaxies are expected to be in this regime, and therefore their detailed kinematics could be used to probe halo triaxiality, one of the basic predictions of the CDM paradigm. We argue that the complex disk kinematics of the dwarf galaxy NGC 2976 might be the reflection of a triaxial halo. Such signatures of halo triaxiality should be common in galaxies where the luminous component is subdominant.

Key words: cosmology: theory – dark matter – galaxies: evolution – galaxies: halos – galaxies: structure – methods: numerical

Online-only material: color figures

1. INTRODUCTION

Cold dark matter (CDM) halos are found to be triaxial in cosmological *N*-body simulations (e.g., Frenk et al. 1988; Dubinski & Carlberg 1991; Jing & Suto 2002; Bett et al. 2007). This finding has motivated a number of studies designed to constrain halo shapes using a variety of probes, including the gravitational lensing of distant galaxies (e.g., Hoekstra et al. 2004; Mandelbaum et al. 2006), the morphology of tidal streams in the Milky Way (MW; e.g., Ibata et al. 2001; Helmi 2004; Law et al. 2009), the kinematics of polar ring galaxies (e.g., Sackett & Sparke 1990), the flaring of galactic disks (e.g., Olling & Merrifield 2000), and the X-ray emission from hot gas in galaxies and clusters (e.g., Kolokotronis et al. 2001; Buote et al. 2002).

Despite these efforts, a clear picture of either conflict or agreement with CDM predictions has yet to emerge. This is in part due to the inherent difficulty of the observational task, but also because most theoretical predictions rely on simulations where the effects of the baryonic component of galaxies are neglected. The assembly of a central galaxy can substantially modify the shape of its surrounding dark halo (see, e.g., Dubinski 1994; Kazantzidis et al. 2004a; Abadi et al. 2010; Tissera et al. 2010) by reshaping the box orbits that sustain triaxiality (e.g., Debattista et al. 2008; Valluri et al. 2010). Although there is reasonable consensus on the qualitative effects of baryons on halo shapes, there has been little quantitative work aimed at gauging the response of realistic triaxial halo models to the changes in the various parameters that characterize the central galaxy, such as its mass, size, or the timescale and mode of its assembly.

Here, we explore these issues using a series of controlled numerical simulations where a triaxial halo is evolved under the influence of a central disk galaxy. Our numerical experiments are similar in nature to those of Dubinski (1994) and Debattista et al. (2008). However, we extend this work in several respects. For example, we focus on the shape of the gravitational potential rather than that of isodensity contours. The potential is less sensitive to the influence of substructures, which can induce substantial but transient changes in the local density while affecting little the overall potential. The gravitational potential is also a quantity of more direct relevance and applicability to many observational studies of halo shapes.

Further, we systematically explore several aspects of the growth of the galaxy that may in principle affect the shape of its surrounding halo. We consider not only the gravitational importance of the disk, but also its orientation relative to the halo principal axes, as well as the timescale and mode of its assembly. Lastly, we use halo parameters in agreement with the results of cosmological *N*-body simulations and galaxy parameters which are consistent with observed scaling laws and span the wide range in surface brightness of observed galaxy disks.

2. SIMULATIONS AND METHODS

We investigate changes in the shapes of triaxial dark matter (DM) halos induced by the growth of central disk galaxies modeled as rigid potentials (see Villalobos et al. 2010 for

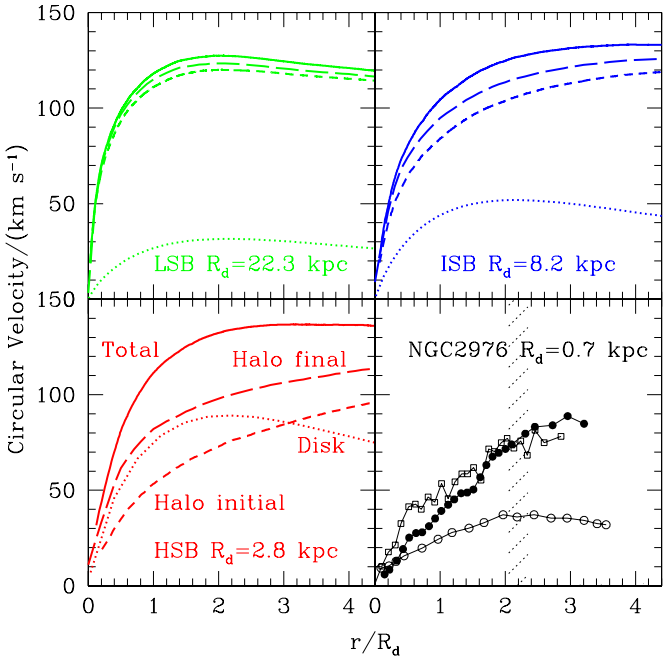

Figure 1. Top and bottom left panels: circular velocity profiles of triaxial halo model A. Short and long dashed lines correspond, respectively, to the halo before and after the addition of the disk (dotted line). The disk mass, in all cases, is $M_d \sim 1.3 \times 10^{10}\,M_\odot$, but its scale length varies: $R_d = 22.3$, 8, and 2.8 kpc. Galaxy masses are consistent with the baryonic TF relation for a rotation speed of $\sim$120 km s^{-1}. The disk models span roughly two decades in surface density (or 5 mag in surface brightness) from values typical of LSB galaxies to intermediate (ISB) to "normal" (HSB) spirals. Radii are given in units of R_d. The halo circular velocity profile peaks at $V_{\rm max} \sim 120$ km s^{-1} at $r_{\rm max} \sim 48$ kpc. Bottom right: circular velocity profile (top two curves) and disk contribution to the circular velocity (bottom curve) for NGC 2976. The disk contribution is taken from Simon et al. (2003). Circular velocities are taken from Simon et al. (2003; filled circles) and Spekkens & Sellwood (2007; open squares). The shaded area indicates the radius, $r = 2.2\,R_d$, where the disk gravitational importance parameter $\eta = V_d/V_{\rm circ}$ is measured. For NGC 2976, $R_d \sim 0.7$ kpc and $\eta \sim 0.5$.

(A color version of this figure is available in the online journal.)

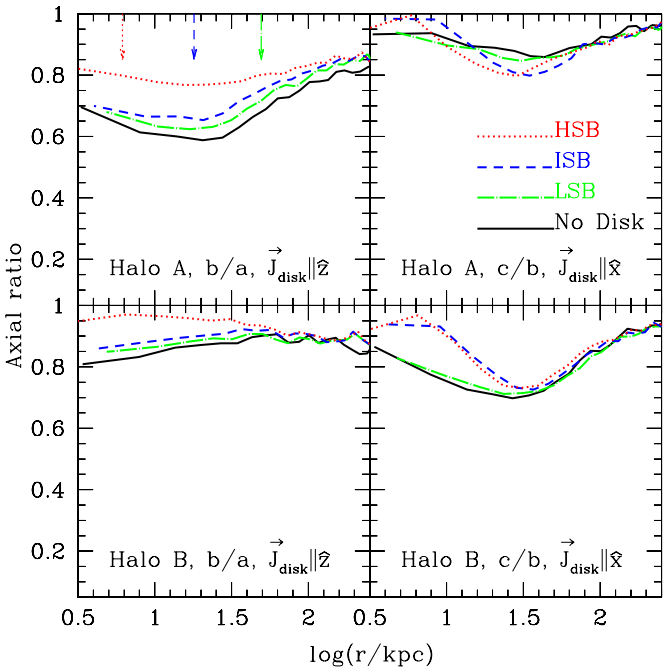

Figure 2. Axial ratios of the halo gravitational potential measured in the plane of the disk before (solid lines) and after the growth of a central galaxy, as a function of radius. Arrows indicate the radius ($r = 2.2\,R_d$) where the disk contribution to the circular velocity is maximum. The dot-dashed, dashed, and dotted lines show halo axial ratios after the growth of the LSB, ISB, and HSB disks, respectively. Panels on the left show the case where the disk plane is perpendicular to the minor (z) axis of the halo, while panels on the right correspond to the case where the disk plane is perpendicular to the major (x) axis of the halo. Results are presented for $\tau_d = 10$ Gyr but are insensitive to τ_d.

(A color version of this figure is available in the online journal.)

details). We measure the shape of the gravitational potential by approximating the isopotential surfaces by ellipsoids and calculating the principal axes a, b, and c (e.g., Springel et al. 2004; Hayashi et al. 2007; Abadi et al. 2010), where a, b, and c denote the major, intermediate, and minor axes, respectively.

The triaxial DM halo models are constructed via successive mergers (Moore et al. 2004). The initial system is a 75,000-particle, isotropic, spherically symmetric model generated by sampling the Hernquist (1990) distribution function (Kazantzidis et al. 2004b). A nearly prolate remnant results from a head-on collision between two such Hernquist models; more triaxial configurations are built by merging this remnant with other Hernquist models on parabolic orbits of various inclinations relative to the principal axes of the first remnant. Each final triaxial halo consists of 300,000 particles. After the mergers are complete, we evolve the remnants for several dynamical times in order to ensure that equilibrium is achieved. The final configurations have mass distributions that can be well approximated by a Navarro–Frenk–White profile (Navarro et al. 1996; in the regions relevant to the present study) and are thus consistent with the results of cosmological CDM simulations.

We adopt two different halo models in order to grow central disks. The first (model A) is a nearly prolate merger remnant, with triaxiality parameter (Franx et al. 1991) $T = (a^2 - b^2)/(a^2 - c^2) \sim 0.8$ for most radii. The second (model B) is strongly triaxial; $T \sim 0.4$ in the inner regions, increasing to $T \sim 0.6$ in the outskirts. These shapes are fairly typical of those found in cosmological simulations (Hayashi et al. 2007). The spin parameters, λ, of halos A and B are 0.024 and 0.040, respectively, which are typical of cosmological halos (Macciò et al. 2008). The circular velocity and axial ratio profiles of these halos are presented in Figures 1 and 2, respectively.

We scale the parameters of halos A and B to match the mass and concentration of CDM halos with maximum circular velocity $V_{\rm max} \sim 120$ km s^{-1}. For a halo of virial mass $M_{\rm vir} = 5 \times 10^{11}\,M_\odot$ and concentration $c \sim 9.3$ (Neto et al. 2007), the circular velocity profile peaks at $r_{\rm max} \sim 48$ kpc.

Disk galaxies forming in our triaxial halos must have rotation speeds comparable to $V_{\rm max}$ in order to satisfy simultaneously the normalization of the Tully–Fisher (TF) relation and the galaxy stellar mass function (see, e.g., Croton et al. 2006; Guo et al. 2010). According to the baryonic TF relation of Noordermeer & Verheijen (2007), the mass of the luminous component of galaxies with rotation speeds of order 120 km s^{-1} is $M_d \sim 1.3 \times 10^{10}\,M_\odot$. We model these galaxies as exponential disks with three different values of the radial scale length, $R_d = 2.8$, 8.0, and 22.3 kpc. (For the disk vertical structure, we assume an isothermal sheet with scale height $z_d = 0.2\,R_d$, consistent with observations of external galaxies.) These values span the range of observed scale lengths for galaxies of this mass, from the very extended low surface brightness (LSB) disks to intermediate surface brightness (ISB) to concentrated high surface brightness (HSB) "normal" spirals.

Within the disk radius the circular speed of the disk+halo system is roughly the same for all models, irrespective of the

surface brightness/density of the disk. This is in agreement with observations, which show that the zero point of the TF relation is roughly independent of surface brightness (Zwaan et al. 1995).

In addition to surface brightness, we have also explored the response of the halo to varying the timescale of disk assembly. This is accomplished by allowing the disk mass to grow linearly over three different timescales, $\tau_d = 0$ Gyr, 1 Gyr, and 10 Gyr. The third choice ensures that the response of the halo is adiabatic, whereas the first, although unrealistic, provides a useful check on the sensitivity of our results to τ_d. We have also varied the mode of disk assembly by simulating cases where the mass of the disk grows in three discrete steps over 1 Gyr, instead of linearly. None of the results we obtain depend on either the choices for τ_d or the mode of disk assembly (see also Berentzen & Shlosman 2006), so we shall mainly concentrate on the "adiabatic" ($\tau_d = 10$ Gyr) experiments where the mass of the disk grows linearly with time.

Because the precise alignment between the disk angular momentum axis and the host halo principal axes is still a matter of debate (e.g., Faltenbacher et al. 2005; Zentner et al. 2005; Bailin et al. 2005), the final parameter we investigated is the orientation of the disk plane relative to the principal axes of the triaxial halo. For each halo, we placed the disk plane perpendicular to its major as well as its minor axis. In total, we performed 24 simulations of the growth of a central disk galaxy in each of the triaxial halo models A and B, for a total of 48 experiments. After the disk growth is complete, all simulations are continued for at least a further 1.5 Gyr in order to allow for equilibrium to be reached. In the experiments where the disk grows in three distinct events, one-third of the disk mass increases instantaneously at 0.1, 0.6, and 1.1 Gyr. We only consider the final equilibrium configurations of the halos when measuring the shape of the potential.

All numerical simulations were carried out with the parallel N-body code PKDGRAV (Stadel 2001). The softening was set to $\epsilon = 0.5$ kpc. Each disk was modeled with $N = 10^5$ static particles in order to ensure a smooth representation of the disk potential.

3. RESULTS

Figure 2 shows the axial ratios of the halo isopotential contours measured in the plane of the disk, for various experiments. The growth of the disk modifies the halo shape, making it more axisymmetric. Halo A is nearly prolate so placing the disk plane perpendicular to the major axis has little effect on the shape of the two-dimensional potential on the disk plane. When the disk plane contains the major axis the potential is strongly non-axisymmetric, but becomes rounder after the disk is added. The effect, however, is minor for the case of the LSB and ISB disks; only the HSB galaxy is able to substantially modify the halo shape, increasing the inner axial ratio from ∼0.6 to ∼0.8.

Before adding the disk, halo B is rather triaxial, with $b/a \sim c/b \sim 0.8$ in the inner regions. In the case of the HSB disk, placing the disk plane perpendicular to the halo minor axis renders the halo potential almost perfectly axisymmetric (measured in the plane of the disk). On the other hand, the LSB and the ISB galaxies are again barely able to modify the shape of the halo. When the disk plane is perpendicular to the halo major axis the results are similar, although in this case the halo response to the ISB and HSB galaxies are comparable. Except very near the center, the potential remains far from axisymmetric in all cases. We note that the change in shape in the case of the HSB disk is noticeable out to ∼30–50 kpc, well outside the region where the disk is gravitationally important.

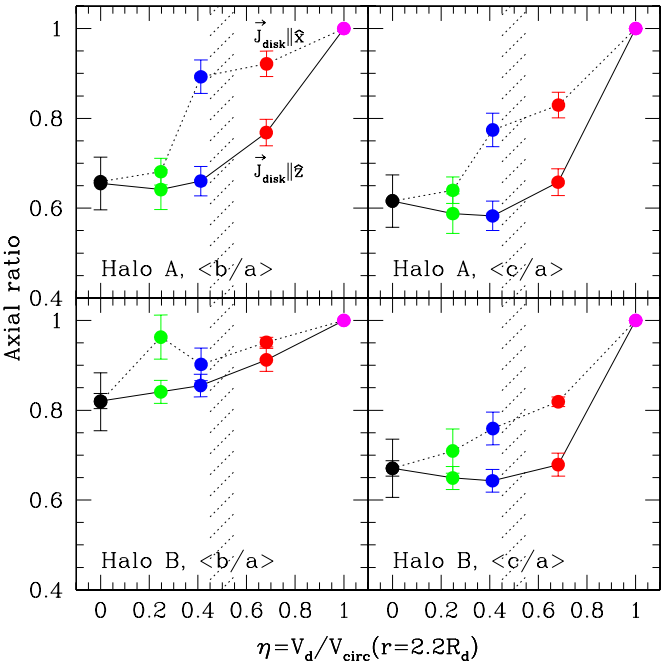

Figure 3. Axial ratios of the inner ($r < 30$ kpc) potential, as a function of the disk gravitational importance parameter, $\eta = V_d/V_{\rm circ}$, measured at $r = 2.2\,R_d$. Symbols and error bars indicate the average and the rms shape of the halo isopotential contours within 30 kpc, respectively. The leftmost point in each panel ($\eta = 0$) corresponds to the halo before adding the disk, while the rightmost point ($\eta = 1$) corresponds to a fully dominant axisymmetric disk. Intermediate values of η show results for disks of different surface density: LSB, ISB, and HSB, from left to right. Results correspond to a disk growth timescale of $\tau_d = 10$ Gyr. The orientation of the disk plane relative to the principal axes of the halo in each panel is indicated in the labels. For given η, the effect is maximal when the disk symmetry axis is aligned with the halo major axis. The shaded area highlights the value of η of NGC 2976.

(A color version of this figure is available in the online journal.)

Figure 3 shows how the three-dimensional halo shape changes in response to the disk growth. The axial ratios of the inner gravitational potential are presented as a function of the peak contribution of the disk to the circular velocity. This is measured by the parameter $\eta = V_d/V_{\rm circ}$, computed at $r = 2.2\,R_d$, the radius where the exponential disk contribution to the circular velocity is maximal. The shape of the potential is not exactly constant in the inner regions (see Figure 2), and therefore we show the shape of the potential averaged inside 30 kpc. The trends we discuss are robust to reasonable changes in the averaging procedure.

Results are presented for the "adiabatic" ($\tau_d = 10$ Gyr) disk growth and for both orientations of the disk plane relative to the halo principal axis. η varies from ∼0.25 for the LSB galaxy to ∼0.7 for the HSB model. Figure 3 demonstrates that in most circumstances the disk growth renders the three-dimensional potential of the halo more spherical. Because halo accelerations are minimal along its major axis, whereas the disk gravity is strongest along its symmetry axis, the effect of a disk on a triaxial halo is maximal when the disk symmetry axis is aligned with the halo major axis, and minimal in the opposite case.

Figures 2 and 3 show that the modifications to halo shapes induced by the disks are relatively minor, except for the HSB galaxy. The response of the halo depends principally on the disk gravitational importance. These results seem insensitive to the timescale and mode of disk assembly. Figure 4 shows

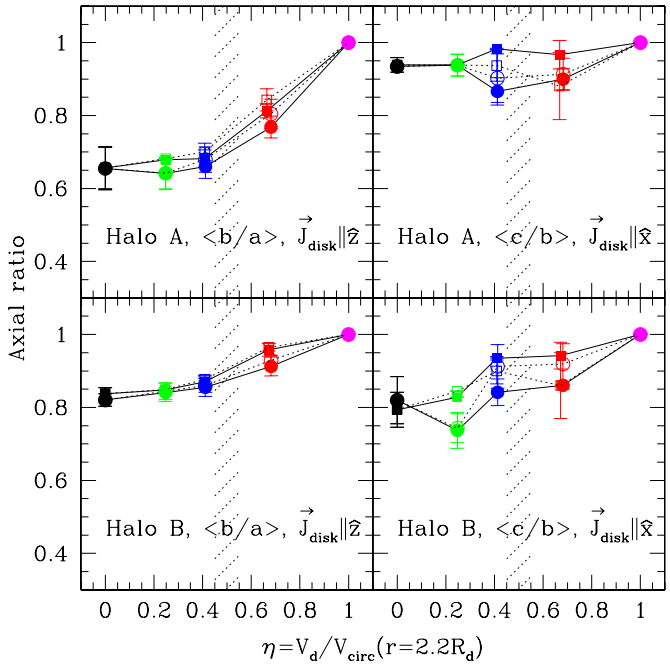

Figure 4. Axial ratios of the inner ($r < 30$ kpc) potential, computed in the plane of the disk, as a function of η. Symbols and error bars are as in Figure 3. Filled symbols show the shape of the halo isopotential contours; open symbols correspond to the total (disk+halo) potential. Circles and squares show cases where the disk growth timescale is $\tau_d = 0$ Gyr and $\tau_d = 10$ Gyr, respectively. The orientation of the disk plane relative to the principal axes of the halo in each panel is as in Figure 2.

(A color version of this figure is available in the online journal.)

this explicitly. This figure shows the axial ratio of the inner potential as a function of η computed in the plane of the disk and confirms the conclusions advanced above. The change in shape is monotonic with η and is relatively minor for the LSB and ISB models. Only the HSB galaxy is able to noticeably modify the halo potential. The transition seems to occur roughly at $\eta \approx 0.5$. Disks that contribute less than about 50% of its circular velocity should be surrounded by halos that have preserved their original triaxiality and, therefore, should in general show signatures of departures from axisymmetry. This is the regime of many LSB and dwarf galaxies, and it is therefore important to consider the possibility that their halos may be triaxial when analyzing their kinematics. Berentzen & Shlosman (2006) also concluded that maximal disks probably reside in nearly axisymmetric halos.

4. DISCUSSION

The sphericalization of DM halos by central galaxies has important implications for the interpretation of observational constraints. For example, a nearly spherical halo is favored by the weak precession of the Sagittarius stream, a result that would be difficult to understand in the CDM paradigm unless the MW halo is an outlier in the distribution of halo shapes (e.g., Ibata et al. 2001; Majewski et al. 2003). Indeed, given the gravitational importance of the MW disk ($\eta \sim 0.8$ for the canonical values of $V_{\rm rot} = 220\,{\rm km\,s^{-1}}$, $R_d = 3$ kpc, and $M_d = 5\times10^{10}\,M_\odot$), the MW halo should have been significantly affected by the disk. Nearly spherical halos may also affect the dynamics of bars and stars in galactic disks (e.g., Ideta & Hozumi 2000; El-Zant & Shlosman 2002) and can inhibit the fueling of nuclear supermassive black holes by suppressing the large-scale asymmetries responsible for the loss of angular momentum in the gas component (e.g., Merritt & Quinlan 1998; Callegari et al. 2010).

On the other hand, our results suggest that LSB halos should retain the triaxiality predicted by cosmological simulations. This may help to explain the rather elongated shapes of the ultra-faint MW satellites (Martin et al. 2008; although these can also be attributed to tidal effects in the gravitational field of the MW) and oddities in the kinematics of some dwarf spheroidal galaxies (see, e.g., Penarrubia et al. 2010). Many dwarf galaxies are also in the regime $\eta 0.5$ where they are unable to modify their surrounding halos. Gaseous disks in such galaxies should exhibit departures from axisymmetry, unless the halos are either prolate or oblate and the disk plane coincides with that where the two-dimensional potential is axisymmetric.

This could indeed be the case in nearly oblate halos, given the preference of the angular momentum to align with the minor axis (Bett et al. 2007). However, in nearly prolate halos (a more common occurrence according to N-body simulations) disks whose angular momentum aligns with the minor axis would feel a non-axisymmetric two-dimensional gravitational potential. Non-circular motions should therefore be fairly common in the gaseous disks of dwarfs, and they could in principle be used to gauge the triaxiality of their surrounding halos.

To first order, a gaseous disk in the non-axisymmetric potential of a triaxial halo would behave just like gas in a barred potential where the pattern speed of the bar is zero. A subdominant disk in a triaxial potential would thus exhibit the non-circular dynamical signature of a (slow) bar but with no obvious bar in the luminous distribution.

Interestingly, there is one system where all these conditions are met. NGC 2976 is a nearby dwarf spiral galaxy whose baryonic disk is subdominant, as shown in the bottom right panel of Figure 1. This figure shows that the contribution of the baryonic component peaks at about one-half of the circular velocity at $r = 2.2\,R_d$ and therefore $\eta \approx 0.5$. Simon et al. (2003) show that the kinematics of the gaseous disk in NGC 2976 is highly complex, exhibiting large non-circular motions near the center. These, according to Spekkens & Sellwood (2007), are best understood as the characteristic kinematic asymmetries imposed by an $m = 2$ bar mode in the gravitational potential (see also Hayashi & Navarro 2006). On the other hand, NGC 2976 has no obvious bar, at least in the optical (but see Menéndez-Delmestre et al. 2007), so ascribing the origin of the non-circular motions to halo triaxiality is clearly tempting.

If this interpretation is correct, then it would be surprising if other galaxies with subdominant baryonic components did not also show signs of being embedded in triaxial potentials. Indeed, one may even argue that the absence of such signatures in a significant fraction of unbarred LSB and dwarf galaxies would be quite difficult to accommodate within the standard CDM paradigm. Definitive conclusions on these issues require more sophisticated theoretical modeling of the formation of subdominant disks in triaxial halos. Note that our models neglect, for example, the response of the disk to the triaxial forcing of the halo as well as a realistic accounting of the distribution of disk orientations relative to the principal axes of the halo. Nevertheless, our results suggest that a careful search for signatures of halo triaxiality in a statistically significant sample of dwarf and LSB galaxies would be warranted. Steps in this direction such as those taken by Trachternach et al. (2009) should certainly be encouraged.

The authors thank Josh Simon and Isaac Shlosman for stimulating discussions. S.K. is supported by the Center for

Cosmology and Astro-Particle Physics (CCAPP) at The Ohio State University. M.G.A. is grateful for the hospitality of CCAPP during the initial stages of this work. This research was supported by an allocation of computing time from the Ohio Supercomputer Center (http://www.osc.edu).

REFERENCES

Abadi, M. G., Navarro, J. F., Fardal, M., Babul, A., & Steinmetz, M. 2010, MNRAS, in press (arXiv:0902.2477)
Bailin, J., et al. 2005, ApJ, 627, L17
Berentzen, I., & Shlosman, I. 2006, ApJ, 648, 807
Bett, P., Eke, V., Frenk, C. S., Jenkins, A., Helly, J., & Navarro, J. 2007, MNRAS, 376, 215
Buote, D. A., Jeltema, T. E., Canizares, C. R., & Garmire, G. P. 2002, ApJ, 577, 183
Callegari, S., Kazantzidis, S., Mayer, L., Colpi, M., Bellovary, J. M., Quinn, T., & Wadsley, J. 2010, ApJ, submitted (arXiv:1002.1712)
Croton, D. J., et al. 2006, MNRAS, 365, 11
Debattista, V. P., et al. 2008, ApJ, 681, 1076
Dubinski, J. 1994, ApJ, 431, 617
Dubinski, J., & Carlberg, R. G. 1991, ApJ, 378, 496
El-Zant, A., & Shlosman, I. 2002, ApJ, 577, 626
Faltenbacher, A., Allgood, B., Gottlöber, S., Yepes, G., & Hoffman, Y. 2005, MNRAS, 362, 1099
Franx, M., Illingworth, G., & de Zeeuw, T. 1991, ApJ, 383, 112
Frenk, C. S., White, S. D. M., Davis, M., & Efstathiou, G. 1988, ApJ, 327, 507
Guo, Q., White, S., Li, C., & Boylan-Kolchin, M. 2010, MNRAS, 404, 1111
Hayashi, E., & Navarro, J. F. 2006, MNRAS, 373, 1117
Hayashi, E., Navarro, J. F., & Springel, V. 2007, MNRAS, 377, 50
Helmi, A. 2004, MNRAS, 351, 643
Hernquist, L. 1990, ApJ, 356, 359
Hoekstra, H., Yee, H. K. C., & Gladders, M. D. 2004, ApJ, 606, 67
Ibata, R., Lewis, G. F., Irwin, M., Totten, E., & Quinn, T. 2001, ApJ, 551, 294
Ideta, M., & Hozumi, S. 2000, ApJ, 535, L91
Jing, Y. P., & Suto, Y. 2002, ApJ, 574, 538
Kazantzidis, S., Kravtsov, A. V., Zentner, A. R., Allgood, B., Nagai, D., & Moore, B. 2004a, ApJ, 611, L73
Kazantzidis, S., Magorrian, J., & Moore, B. 2004b, ApJ, 601, 37
Kolokotronis, V., Basilakos, S., Plionis, M., & Georgantopoulos, I. 2001, MNRAS, 320, 49
Law, D. R., Majewski, S. R., & Johnston, K. V. 2009, ApJ, 703, L67
Macciò, A. V., Dutton, A. A., & van den Bosch, F. C. 2008, MNRAS, 391, 1940
Majewski, S. R., Skrutskie, M. F., Weinberg, M. D., & Ostheimer, J. C. 2003, ApJ, 599, 1082
Mandelbaum, R., Hirata, C. M., Broderick, T., Seljak, U., & Brinkmann, J. 2006, MNRAS, 370, 1008
Martin, N. F., de Jong, J. T. A., & Rix, H. 2008, ApJ, 684, 1075
Menéndez-Delmestre, K., Sheth, K., Schinnerer, E., Jarrett, T. H., & Scoville, N. Z. 2007, ApJ, 657, 790
Merritt, D., & Quinlan, G. D. 1998, ApJ, 498, 625
Moore, B., Kazantzidis, S., Diemand, J., & Stadel, J. 2004, MNRAS, 354, 522
Navarro, J. F., Frenk, C. S., & White, S. D. M. 1996, ApJ, 462, 563
Neto, A. F., et al. 2007, MNRAS, 381, 1450
Noordermeer, E., & Verheijen, M. A. W. 2007, MNRAS, 381, 1463
Olling, R. P., & Merrifield, M. R. 2000, MNRAS, 311, 361
Penarrubia, J., Walker, M. G., & Gilmore, G. 2010, in AIP Conf. Ser. 1240, Hunting for the Dark: The Hidden Side of Galaxy Formation, ed. V. P. Debattista & C. C. Popescu (Melville, NY: AIP), 375
Sackett, P. D., & Sparke, L. S. 1990, ApJ, 361, 408
Simon, J. D., Bolatto, A. D., Leroy, A., & Blitz, L. 2003, ApJ, 596, 957
Spekkens, K., & Sellwood, J. A. 2007, ApJ, 664, 204
Springel, V., White, S. D. M., & Hernquist, L. 2004, in IAU Symp. 220, Dark Matter in Galaxies, ed. S. Ryder et al. (Cambridge: Cambridge Univ. Press), 421
Stadel, J. G. 2001, PhD thesis, Univ. Washington
Tissera, P. B., White, S. D. M., Pedrosa, S., & Scannapieco, C. 2010, MNRAS, 406, 922
Trachternach, C., de Blok, W. J. G., McGaugh, S. S., van der Hulst, J. M., & Dettmar, R. 2009, A&A, 505, 577
Valluri, M., Debattista, V. P., Quinn, T., & Moore, B. 2010, MNRAS, 403, 525
Villalobos, Á., Kazantzidis, S., & Helmi, A. 2010, ApJ, 718, 314
Zentner, A. R., Kravtsov, A. V., Gnedin, O. Y., & Klypin, A. A. 2005, ApJ, 629, 219
Zwaan, M. A., van der Hulst, J. M., de Blok, W. J. G., & McGaugh, S. S. 1995, MNRAS, 273, L35